Enzyme and Microbial Technology 60 (2014) 24–31

Contents lists available at ScienceDirect

Enzyme and Microbial Technology

journal homepage: www.elsevier.com/locate/emt

# Chemotherapy pro-drug activation by biocatalytic virus-like nanoparticles containing cytochrome P450

Lorena Sánchez-Sánchez [a], Rubén D. Cadena-Nava [b], Laura A. Palomares [a], Jaime Ruiz-Garcia [c], Melissa S.T. Koay [d], Jeroen J.M.T. Cornelissen [d], Rafael Vazquez-Duhalt [a,b,*]

[a] Institute of Biotechnology, Universidad Nacional Autónoma de México, Cuernavaca, Morelos, Mexico
[b] Center for Nanosciences and Nanotechnology, Universidad Nacional Autónoma de México, Ensenada, Baja California, Mexico
[c] Institute of Physics, Autonomous University of San Luis, San Luis Potosi, SLP, Mexico
[d] Department of Biomolecular Nanotechnology, MESA Institute of Nanotechnology, University of Twente, The Netherlands

ARTICLE INFO

*Article history:*
Received 13 January 2014
Received in revised form 11 March 2014
Accepted 2 April 2014
Available online 13 April 2014

*Keywords:*
Bionanotechnology
CYP
Catalytic VLPs
Tamoxifen
Resveratrol

ABSTRACT

This work shows, for the first time, the encapsulation of a highly relevant protein in the biomedical field into virus-like particles (VLPs). A bacterial CYP variant was effectively encapsulated in VLPs constituted of coat protein from cowpea chlorotic mottle virus (CCMV). The catalytic VLPs are able to transform the chemotherapeutic pro-drug, tamoxifen, and the emerging pro-drug resveratrol. The chemical nature of the products was identified, confirming similar active products than those obtained with human CYP. The enzymatic VLPs remain stable after the catalytic reaction. The potential use of these biocatalytic nanoparticles as targeted CYP carriers for the activation of chemotherapy drugs is discussed.



## 1. Introduction

Despite significant advances toward the development and improvement of more effective anticancer therapies, the cancer is still an unsolved problem [1]. Nowadays, chemotherapy is the most used strategy to fight cancer tumors [2]. There are more than 100 different cytotoxic drugs currently available and new ones are being developed all the time. Although chemotherapy without a doubt has helped to save millions of lives, the associated systemic side effects are a main drawback. The cytotoxic drugs used in chemotherapy do not recognize the difference between fast-growing cancer cells and other types of fast-growing cells. These include blood cells, skin cells, the cells on the scalp and the cells inside the stomach [3]. Consequently, most chemotherapy medications have a poisonous effect on the healthy body's cells. The ability to control drug delivery and its subsequent release at the site-specific location remains a major challenge.

A great diversity of chemical compounds is being used as chemotherapeutic agents [4]. Most of them are administered as pro-drugs and thus they have to be activated into the potent anti-carcinogenic drug, a task performed mainly by the cytochrome P450 superfamily [4]. The majority of these pro-drugs are activated in the liver, where CYPs (especially families 1–3) are overexpressed [5], inducing the capacity to transform exogenous compounds. Unfortunately, the CYP expression varies significantly in the different tissues [6], and even more, in some cases the healthy cells near to the tumor cells express higher CYP activity [7], preferentially activating the cytotoxic agent, and affecting these healthy cells.

Several strategies aim toward increasing the *in situ* generation of the active form of the drug within the tumor. By increasing the CYP activity in the tumor tissue, chemotherapeutic treatment would be more efficient and the amount of drug administered could be lowered thereby reducing the toxic systemic side effects. Emerging strategies such as gene-directed enzyme pro-drug therapy (GDEPT) [8] and virus-directed enzyme pro-drug therapy (VDEPT) [9,10] aim to promote the tumor-specific activation of the pro-drugs by using gene therapy to sensitize tumor cells to anticancer pro-drugs. A promising alternative, to overcome the problems associated with the insertion and expression of genes in human (mammalian) cells, is to deliver directly the enzyme to specific targets *via* virus-like particles (VLPs). Composed of an outer protein shell (capsid) that

* Corresponding author at: Centro de Nanociencias y Nanotecnología, UNAM, Km 107 Carretera Tijuana-Ensenada, Ensenada, Baja California 22800, Mexico. Tel.: +52 6461750650.
*E-mail addresses:* rvd@cnyn.unam.mx, vazqduh@hotmail.com (R. Vazquez-Duhalt).

http://dx.doi.org/10.1016/j.enzmictec.2014.04.003
0141-0229/

surrounds its genomic RNA/DNA, the genomic cargo of viruses can be removed and the outer capsid can be reassembled to form empty virus-like particles (VLPs) that resemble the morphology of native viruses. Devoid of its native cargo, the internal cavity of empty VLPs has been explored extensively for the encapsulation of metals [11], polymers [12], proteins [13,14], enzymes [15,16], DNA [17], drugs [18] and therapeutic agents [19,20]. VLPs offer distinct advantages as molecular cargo vehicles since they [21–23]; (i) possess high payload capacity; (ii) bear multiple sites that can be readily functionalized for cell-specific targeting; (iii) are inherently designed to protect and deliver molecular cargo to a target; and (iv) could be accumulated within solid tumors due to nanometer size (enhanced permeability and retention effect). Protein encapsulation in viral capsids, called "encapsidation" because they are perfectly structured, has been mainly focused on trapping fluorescent proteins inside protein cages [13,14,24]. Until recently, few examples of encapsulated enzymes inside VLPs, and other protein structures, have been reported in order to obtain nanobioreactors [15,16,25–28]. However, the use of virus-like particles as CYP enzyme carriers for pro-drug therapy has scarcely been reported.

In this work, $CYP_{BM3}$ from *B. megaterium*, mutant "21B3" has been used as a model for the encapsulation of CYPs in VLPs. This variant, with improved peroxygenase activity, gives us an operational advantage since it uses hydrogen peroxide instead of the expensive cofactor NADPH [29]. Moreover, this CYP is stable and soluble in aqueous media and it can be produced in large quantities, as opposed to human CYPs. $CYP_{BM3}$ has proven to be a versatile enzyme that can be engineered, by rational design or directed evolution [30], to transform a great variety of non-natural substrates, including several drugs usually metabolized by human CYPs [31]. These characteristics make it a very promising enzyme for therapeutic applications.

The aim, and innovation, of this work is to demonstrate the potential use of virus-like nanoparticles derived from a plant virus as carriers to deliver CYP enzymatic activity. These nanoparticles could be targeted to the tumor cells by chemical functionalization increasing the pro-drug activation in specific sites, reducing the doses needed and the side effects associated with chemotherapy.

## 2. Materials and methods

### 2.1. Chemicals

Pro-drugs, 7-pentoxyresorufin, 2,6-dimethoxyphenol, isopropyl β-D-thiogalactoside (IPTG), acetic acid and hydrogen peroxide (30% w/w) were purchased from Sigma–Aldrich (Milwaukee, WI). HPLC-grade organic solvents (acetonitrile and methanol) were obtained from Burdick & Jackson (Honeywell). Glacial acetic acid ACS was obtained from Fermont (Shakopee, MN). Buffer salts were purchased from J.T. Baker (Phillipsburg, NJ).

### 2.2. Expression and purification $CYP_{BM3}$ 21B3

The plasmid pCWori encoding for the heme domain of the $CYP_{BM3}$ 21B3 was a kind gift from Prof. Frances Arnold from the California Institute of Technology (Caltech). $CYP_{BM3}$ mutant 21B3 was expressed in *Escherichia coli* DH5α using the β-D-thiogalactopyranoside (IPTG)-inducible pCWori vector. Cultures for protein production were grown as described by Cirino and Arnold [29].

The $CYP_{BM3}$ 21B3 purification was performed by chromatography in an EconoSystem from Bio-Rad® equipped with a 5 mL Ni-pre-charged HisTrap HP column (Amersham Biosciences®). The equilibration buffer consisted in 50 mM $NaH_2PO_4$, 300 mM NaCl and 10 mM imidazole, pH 8. The protein mixture was loaded at 1.5 mL $min^{-1}$. The CYP protein was eluted in a buffer containing 300 mM imidazole at 3 mL/min for 10 min. The colored fractions were collected, concentrated by ultrafiltration and stored at −20 °C in 50 mM Tris–HCl buffer, pH 8, containing 10% glycerol. CYP-protein concentration was determined by using the Bradford BioRad protein assay. The production of purified $CYP_{BM3}$ 21B3 reached 50 mg of enzyme per liter of culture with 91% purity as estimated by SDS–PAGE electrophoresis.

### 2.3. CCMV expression and purification

The pET15b plasmid encoding wild-type capsid protein of Cowpea Chlorotic Mottle Virus (CCMV), bearing an N-terminal hexahistidine-tag was transformed into *Escherichia coli* BL21(DE3)pLysS (Novagen) for protein expression. Starting cultures were grown overnight at 37 °C from glycerol stock cells in 7 mL of LB medium (Sigma–Aldrich) containing 100 μg/mL ampicillin and 34 μg/mL chloramphenicol (Sigma–Aldrich). Overnight cultures were used to inoculate 0.5 L LB medium containing ampicillin (100 μg/mL) and chloramphenicol (34 μg/mL) and grown to an optical density of $OD_{600} = 0.6 \pm 0.08$.

Protein expression was induced following addition of IPTG to a final concentration of 0.1 mM at 30 °C for 5 hours. The cells were harvested by centrifugation (10,000 × *g* for 15 min) and lysed using BugBuster according to the manufacturer protocol (Novagen). Wild-type CCMV bearing the N-terminal His-tag was purified using nickel affinity column chromatography with a modified version of the supplier protocol (Novagen). Upon protein binding (in 0.1 M phosphate buffer, 0.3 M NaCl, 5 mM imidazole at pH 8.0), weakly bound and other unwanted proteins were washed with 5 column volumes of 0.1 M phosphate buffer, 0.3 M NaCl and 12.5 mM imidazole at pH 8.0 before washing with 10 column volumes of 0.1 M phosphate buffer, 1.5 M NaCl, 12.5 mM imidazole at pH 8.0 to remove bound RNA. The desired protein was eluted with 0.1 M phosphate buffer, 1.5 M NaCl, 0.25 M imidazole at pH 8.0 before dialyzing overnight to 50 mM Tris–Cl buffer, 0.5 M NaCl, 10 mM $MgCl_2$, 1 mM ethylenediamine-tetraacetic acid (EDTA), pH 7.5 to remove excess imidazole. Then, the purified His-tag CCMV was dialyzed to 50 mM sodium acetate buffer, 1 M NaCl and, 1 mM $NaN_3$ (pH 5.0) to induce capsid formation. The assembled capsids were purified and analyzed by FPLC using a Superose 6 column.

### 2.4. CYP encapsulation inside CCMV capsids

First, CCMV empty capsids (at 1 mg $mL^{-1}$) were dialyzed against disassembly buffer (20 mM Tris–Cl, 1 M NaCl, pH 7.2) for 48 h at 4 °C to obtain dissociated CCMV protein [32]. CYP encapsulation was tested at different CCMV:CYP ratios. The capsid assembly of protein CCMV in the presence of CYP was performed in assembly buffer (50 mM Tris–HCl, 50 mM NaCl, 10 mM KCl, 5 mM $MgCl_2$, pH 7.2) at the following CCMV:CYP molar ratios: 4:1, 12:1 and 20:1. For all samples, the enzyme concentration was kept constant (2.25 μM). After an overnight assembly at 4 °C, the extent of encapsulation and the formation of VLPs were analyzed by agarose gel electrophoresis. A 10 μL aliquot of each ratio was mixed with 3 μL of 100% glycerol and loaded into a 1% agarose gel (BioRad) in electrophoresis buffer (0.1 M sodium acetate, 1 mM EDTA, pH 6). The samples were ran for 3 h at 65 V at 4 °C before staining with InstantBlue (Expedeon) for 1 h.

For the production of catalytic VLPs, dissociated CCMV protein monomers and CYP (2.25 μM) were mixed at a molar ratio of 12:1 at a final reaction volume of 300 μL and then dialyzed for 16 h at 4 °C against assembly buffer. The sample was loaded on a 100 kDa Amicon centrifuge filter (0.5 mL) and centrifuged for 5 min at 7000 × *g* at 4 °C. The sample was washed five times with assembly buffer to remove the free CYP and any unassembled CCMV protein. Then, the sample was concentrated to a final volume of 50 μL. A 5 μL aliquot was loaded on a 12% SDS-PAGE gel to verify the integrity of both proteins, CCMV and CYP, and the proportion of encapsulation was estimated by densitometry.

### 2.5. Transmission electron microscopy analysis of VLPs

The VLPs were applied to 200 mesh copper Formvar grids (Electron Microscopy Science) and then negatively stained. A 6 μL aliquot of VLP's (diluted 3.5-times) was spread onto the grid for 1 min, blotted with Whatman filter paper, and then stained with 6 μL of 2% uranyl acetate for 1 min. Excess stain was removed by blotting with filter paper. The samples were analyzed with a JEOL JEM-2010 transmission electron microscope operated at 200 keV and equipped with a wide-angle (top mount) BioScan 600-W 1 × 1 K pixel digital camera. The average diameter of the VLPs was obtained with the software ImageJ (U.S. National Institutes of Health) and was calculated as the geometric mean of two orthogonal measurements of the capsids.

### 2.6. Enzymatic activity determination of CYP

The enzyme activity on 7-pentoxyresorufin-O-deethylase (PROD) was determined monitoring the fluorescent O-dealkylation product in a Safire (Tecan) microplate fluorimeter with an excitation wavelength of 530 nm and emission wavelength of 585 nm. The product of the reaction was quantified using a resorufin standard curve (5–500 nM). All reactions were performed in 50 mM Tris–HCl buffer (pH 8) at 25 °C and initiated by adding 5 mM of $H_2O_2$. The activity on 2,6-dimethoxyphenol was monitored spectrophotometrically at 468 nm ($\varepsilon$ = 14,800 $M^{-1}$ $cm^{-1}$) using a Perkin Elmer Lambda 25 UV/VIS spectrophotometer.

### 2.7. CYP pro-drug transformation

The enzymatic transformation of tamoxifen, resveratrol, tegafur, dacarbazine, ifosfamide and cyclophophamide by $CYP_{BM3}$ 21B3 was performed in a 100 mM phosphate buffer (pH 7.4) at 25 °C for 15 min. For tegafur, the reaction mixture (0.25 mL) contained 50 μM of tegafur and 0.6 nmol of CYP and the HPLC analysis was performed as reported by Komatsu et al. [33]. For dacarbazine, the reaction mixture (0.5 mL) contained 500 μM of dacarbazine and 1.2 nmol of CYP and the analysis was performed according to Lewis et al. [34]. For ifosfamide and cyclophosphamide, the reaction mixture (1.0 mL) contained 5 mM of substrate and 3 nmol of CYP and the pro-drug transformation was monitored by HPLC [35]. For tamoxifen and resveratrol, the kinetic constants were determined varying the substrate concentration until saturation, as described in the next section. All pro-drug transformation reactions were initiated by adding 5 mM $H_2O_2$. The enzymatic activity for each substrate was determined on a HPLC chromatograph (Agillent serie 1100) equipped with a Kinetex reverse phase column $C_{18}$, 5 μm (Phenomenex, CA).

### 2.8. Determination of kinetic constants

The kinetic parameters for tamoxifen and resveratrol were calculated based on substrate disappearance and monitored by HPLC. The $k_{cat}$ and $K_M$ values were obtained by fitting the data to a Michaelis–Menten plot using the software Sigma Plot 11.0 (Systat Software, Inc.). All reactions were performed at 25 °C.

#### 2.8.1. Tamoxifen

The reaction mixture (final volume of 0.5 mL) contained between 20 and 200 μM tamoxifen and CYP (90–225 pmol) in a 100 mM potassium phosphate buffer (pH 7.4) containing 1% methanol and 2 mM ascorbic acid. The reactions were initiated by adding 5 mM $H_2O_2$ and carried out at 25 °C for 5 min, and then the reaction was stopped by adding 50 μL of acetic acid. The samples were centrifuged and analyzed by the HPLC with an elution gradient (0.75 mL $min^{-1}$) from 10 mM ammonium acetate (pH 3) to 65% acetonitrile in 10 min, and monitored at 280 nm.

#### 2.8.2. Resveratrol

The reaction mixture (0.25 mL) contained from 30 to 200 μM resveratrol and 50 pmol of CYP in a 100 mM potassium phosphate buffer (pH 7.4) containing 0.5% of dimethylsulfoxide. Reactions were carried out at 25 °C for 5 min and stopped by adding an equal volume of acetonitrile. The samples were then centrifuged and analyzed by HPLC. Resveratrol, and its metabolites, were separated by isocratic elution (0.65 mL $min^{-1}$) with 25% acetonitrile in water containing 0.1% acetic acid, and monitored at 320 nm.

### 2.9. Analysis of the transformation products

The enzymatic reactions for tamoxifen and resveratrol were performed in 0.5 mL. All mass spectral analyses were performed at the Queen's Mass Spectrometry and Proteomics Unit (MSPU) at the Queen's University in Kingston, Ontario. The reaction mixture for tamoxifen contained: 80 μM tamoxifen, 1.8 nmol CYP and 5 mM $H_2O_2$ in 50 mM Tris–HCl (pH 7.4). The reaction mixture for resveratrol contained: 100 μM resveratrol, 0.6 nmol CYP and 5 mM hydrogen peroxide in 50 mM Tris–HCl (pH 7.4). Both reactions were held for 20 min and then stored at −20 °C. The reaction products were analyzed by LC/MS/MS in a QStar XL QqTOF equipped with a NanoESI source and Agilent capillary HPLC 1100 system with a mass resolution of 10,000 Da and a mass accuracy of 5 ppm for organic compounds. The samples were eluted with a gradient from 0.1% formic acid in water to 0.1% formic acid in acetonitrile in 25 min at a rate of 300 nL $min^{-1}$.

### 2.10. Activity in CCMV-CYP virus-like particles

The catalytic activity determination of CYP-containing VLPs was performed with tamoxifen as a substrate. The reaction mixture (0.1 mL) contained 140 μM tamoxifen, ∼58 pmol of encapsulated CYP in a 100 mM potassium phosphate buffer (pH 7.4) with 2 mM ascorbic acid. The reaction was started with 5 mM $H_2O_2$ and held for 30 min at 25 °C, and finally stopped by adding 10 μL of acetic acid. The sample was centrifuged and analyzed by HPLC as previously described.

## 3. Results and discussion

Initially, the ability of $CYP_{BM3}$ 21B3 to activate the well-known chemotherapeutic pro-drugs tamoxifen, dacarbazine, ifosfamide, cyclophosphamide, tegafur and the emerging pro-drug resveratrol was determined. Tamoxifen and resveratrol are both efficiently transformed whereas no transformation could be detected for the other four pro-drugs assayed under the reaction conditions tested. The kinetic constant of tamoxifen and resveratrol were determined (Table 1). In addition to pro-drugs, a substrate for CYPs, 7-pentoxyresorufin (PROD), and a substrate for peroxidases, 2,6-dimethoxyphenol, were assayed too. Tamoxifen, resveratrol and 2,6-dimethoxyphenol were relatively good substrates for $CYP_{BM3}$ 21B3, while PROD showed a low catalytic rate. Despite a lower $K_M$ (119 μM), our $CYP_{BM3}$ 21B3 mutant showed one order of magnitude improved for the resveratrol transformation activity, $k_{cat}$ (69.8 $min^{-1}$), compared with the variant reported by Kim et al. [36], suggesting a slightly enhanced catalytic efficiency.

The products from the enzymatic transformation of tamoxifen and resveratrol were analyzed on a high performance hybrid quadrupole time-of-flight mass spectrometer (LC–MS–MS) with a Fourier Transform Mass Spectrometry analyzer (FT-MS) (Fig. 1). N-desmethyltamoxifen, 3,4′-dihydroxytamoxifen, endoxifen and 4-hydroxytamoxifen were identified from the tamoxifen transformation with $CYP_{BM3}$ 21B3 in the presence of 5 mM of hydrogen peroxide. From the $CYP_{BM3}$ 21B3 transformation of resveratrol the main product was determined to be piceatannol. Thus, the transformation of a series of structurally different chemotherapeutic pro-drugs and its capacity to transform them into the metabolically active drugs was confirmed. $CYP_{BM3}$ 21B3 is capable of performing hydroxylations on the aromatic rings of tamoxifen and resveratrol, as well as N-demethylation on tamoxifen.

Tamoxifen is the most widely used pro-drug in the treatment of hormone-dependent breast cancer [37]. It acts as a selective estrogen receptor modulator, ultimately reducing or eliminating the proliferation of the tumor cells [38]. CYPs, mainly in the liver, are involved in the tamoxifen metabolism, producing the active drugs. $CYP_{BM3}$ 21B3 was able to generate the two pharmacologically active metabolites, 4-hydroxytamoxifen and endoxifen (4-hydroxy N-demethyltamoxifen) [39]. The N-demethyltamoxifen is an intermediate compound in the generation of endoxifen. On the other hand, the dihydroxylated product 3,4′-dihydroxytamoxifen (or 4,4-dihydoxytamoxifen) is a reactive species that covalently binds to DNA and proteins, that could increase the toxic effects [40].

The long-term usage of tamoxifen, causes severe damage to other tissues in the organism, limiting the duration of the therapy to no more than 5 years [41]. Pro-drug activation at the specific tumor site *via* VLPs containing CYP activity could significantly decrease the required doses and treatment-time needed to achieve the therapeutic effect, and thus reducing the severe associated side effects. Another important drawback is the existence of a great amount of polymorphisms in the CYP2D6 gene, the main CYP involved in the generation of endoxifen [42]. Delivering CYP enzymatic activity to the tumor sites of individuals with impaired metabolism of CYP2D6 could be especially useful to increase the efficacy of the treatment.

On the other hand, the main product of the $CYP_{BM3}$ 21B3 transformation of resveratrol, a known cancer chemopreventive agent [43] was piceatannol. Among other biological activities [44], piceatannol has been implicated as an important anticarcinogen by suppressing proliferation of cancer cells [45] and inducing apoptosis [46]. These activities make piceatannol a potentially interesting drug for cancer treatment.

The $CYP_{BM3}$ 21B3 showed the highest catalytic activity with the 2,4-dimethoxyphenol confirming its high peroxidase activity

**Table 1**
Kinetic constant for the $CYP_{BM3}$ 21B3 mediated transformation of pro-drug compounds and CYP substrates.

| Substrate | $k_{cat}$ ($min^{-1}$) | $K_M$ (μM) | $k_{cat}/K_M$ ($min^{-1}$ $μM^{-1}$) |
|---|---|---|---|
| Tamoxifen | 41.9 (±4.2) | 106.9 (±23.01) | 0.392 |
| Resveratrol | 69.8 (±11.4) | 119.0 (±39.8) | 0.586 |
| PROD | 0.0012 (±0.00024) | 1.37 (±0.12) | 0.00087 |
| 2,6-Dimethoxyphenol | 141.2 (±3.7) | 23.7 (±2.7) | 5.958 |

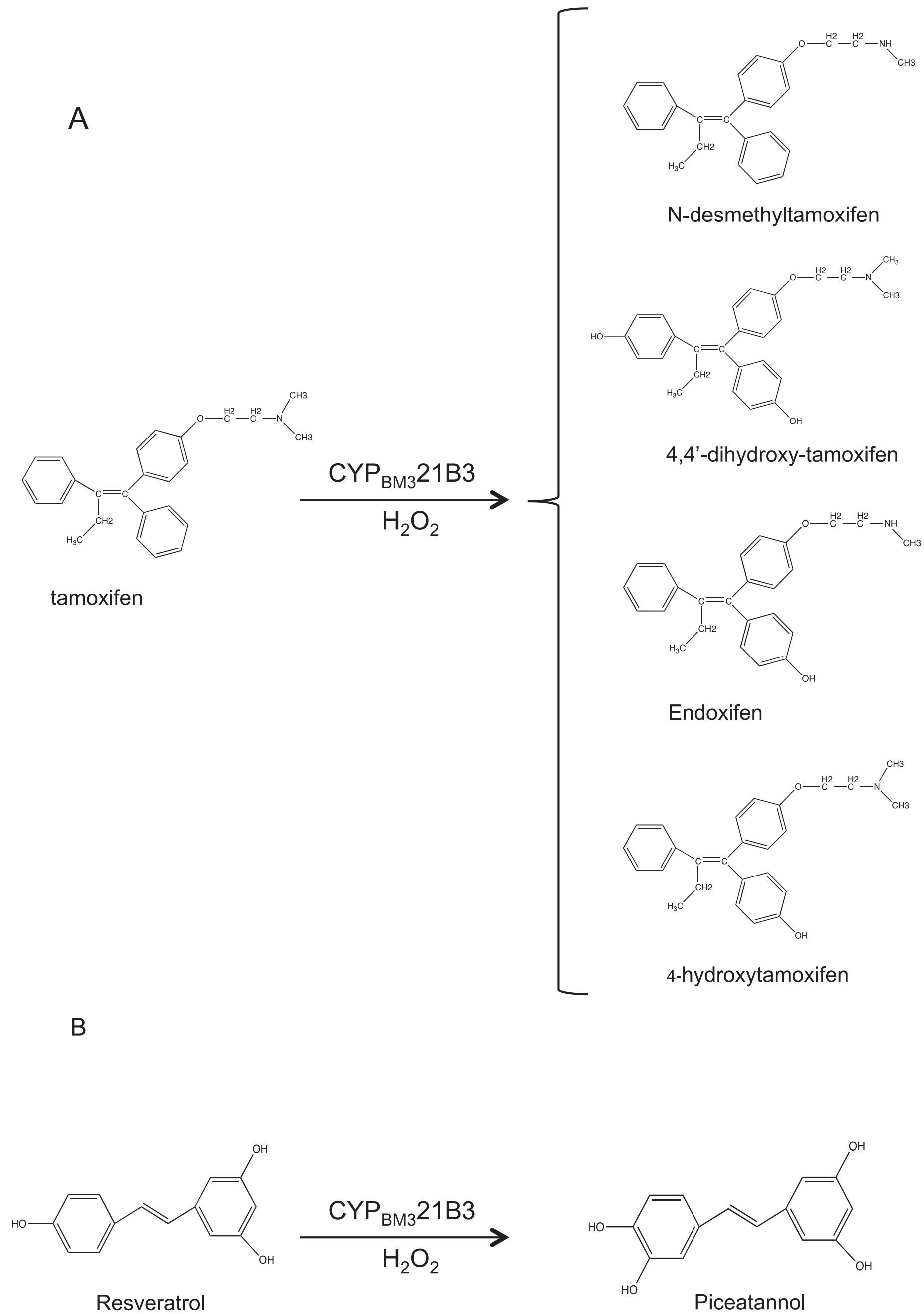


**Fig. 1.** $CYP_{BM3}$ 21B3 pro-drug reaction products. (A) Structure of tamoxifen and its active metabolites and (B) resveratrol and its active metabolite.

[29]. On the other hand, $CYP_{BM3}$ 21B3 showed also activity in the PROD assay, but in a less extent. MROD, EROD and BROD were also assayed giving less turnover rates than PROD (data not shown). The O-dealkylations of 7-alkoxyresorufins are widely used as activity probes for measuring the cytochrome P450 isoforms [47]. Nevertheless, there is considerable inter-individual variation in the involvement of different P450 forms in O-dealkylations of 7-alkoxyresorufins in human liver, and these substrates are not strictly specific for each CYP family [47]. Although the rate of conversion to resorufin was slow, the low detection limit of the product makes it a sensitive method when low concentration of enzyme is used.

The CCMV VLPs were disassembled and then reassembled in the presence of CYP. The encapsulation of $CYP_{BM3}$ 21B3 inside CCMV VLPs is driven *via* complementary electrostatic charges between the negatively charged $CYP_{BM3}$ cargo and the positively charged N-termini of the CCMV capsid protein [48] (Fig. 2). Different molar ratios of CCMV coat protein to CYP were tested (4:1, 12:1 and 20:1), whilst maintaining the enzyme concentration constant (2.25 μM). We have found encapsulation at the three molar ratios assayed. Nanostructure formation was monitored by an electrophoretic mobility shift assay (EMSA) on agarose gel (Fig. 3A), in which there is a clear migration shift in the electrophoretic mobility of the CCMV protein as consequence of the presence of the associated CYP in all three molar ratios assayed. The difference in the migration between the encapsulation at the different molar ratios could be attributed in part, to a difference in the amount of enzyme internalized, but also to an increase in the nanotube population as a result of higher initial concentrations of CCMV coat proteins, this migration shift also has been observed when RNA is encapsulated [32]. As can be seen from transmission electron microscopy (TEM) images (Fig. 3B) there are VLPs present at the CCMV-CYP 4:1, 12:1 and 20:1 molar ratios.

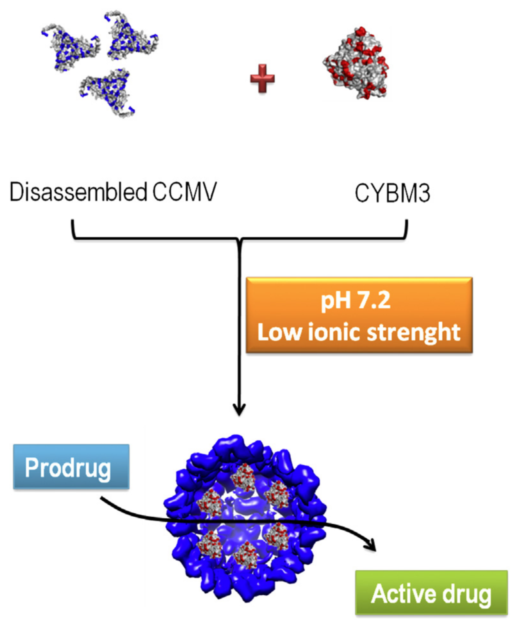


**Fig. 2.** Schematic representation of $CYP_{BM3}$ encapsulation inside CCMV VLP. The internalization of the enzyme was favored by complementary electrostatic interactions between the negatively charged CYP (red) and the positively charged interior of the capsid (blue). The overall net charge of $CYP_{BM3}$ 21B3 was −12 (calculated with the software Maestro version 9.3, Schrödinger, Inc.). (For interpretation of the references to color in this figure legend, the reader is referred to the web version of the article.)

Uranyl acetate internalization was not observed in the preparations with CYP, as opposed to empty CCMV capsids, suggesting that the VLPs contain encapsulated CYP. At high initial concentrations of CCMV coat protein (27 and 45 μM) the presence of some rod-like structures was also observed. These tubular structures were present only at the 27:1 and 45:1 molar ratios, with a higher population and sizes when using a starting concentration of 45 μM capsid protein. The formation of nanotubes has been previously reported for empty CCMV VLPs under neutral pHs and low ionic strengths [49], which correspond close to the assembly conditions used in this work. The nature and size of the molecules placed inside also play a role in defining the shape and size of CCMV structures [12,32,50].

To minimize the presence of rod-like structures, the VLPs derived from the 12:1 coat protein:CYP ratio were further characterized. This CCMV-CYP ratio generates well defined structures with a majority of spheres as confirmed by TEM (Fig. 4A). The spherical VLPs showed an average diameter of 27 ± 2.4 nm, although a very few rod-like assemblies of varying lengths ranging from 40 to 170 nm were also observed with an average diameter of 20.8 ± 1.7 nm (Fig. 4A). The presence of CYP in the VLPs of CCMV was further demonstrated by SDS–PAGE electrophoresis (Fig. 4B). The number of enzymes packaged per particle was determined by densitometry analysis, indicating an average of 14 $CYP_{BM3}$ 21B3 molecules per CCMV capsid, which corresponds to an effective enzyme concentration of 4.9 mM (considering an internal CCMV volume of $4.7 \times 10^{-21}$ L). As seen by TEM (Fig. 4A), the packaging of CYP inside CCMV did not affect the capsid structure. The diameter of the nanospheres (with icosahedral symmetry) is very similar to the reported for native virus (28 nm) corresponding to a triangulation number of $T = 3$ icosahedral state [51].

The occupancy of the CCMV capsid with enzyme is around 45% of the available volume. The theoretical value of CYPs (150 $nm^3$) per capsid is around 31 enzyme molecules per CCMV. Since the encapsulation involved only the interaction of the internal surface of the virus with the enzyme it is expected not to be able to reach this maximum. However, with our strategy we were able to encapsulate one of the greatest numbers of cargo protein reported for this capsid [26].

The CCMV VLP has been extensively used to package different types of molecules ranging from metallic nanoparticles [48] to synthetic polymers [52]. The CCMV capsid formation is highly favored by the presence of stabilizing molecules with negative charge such as nucleic acids and other polyelectrolytes. In this work, the driving force directing the selective encapsulation of CYP inside the CCMV capsid is based on complementary electrostatic interactions between the positively charged interior by the N-terminus of the CCMV capsid protein and the negatively charged surface of CYP, at neutral pH. It is worth saying that the exterior of the capsid is negatively charged, making unlikely the interaction of the enzyme with

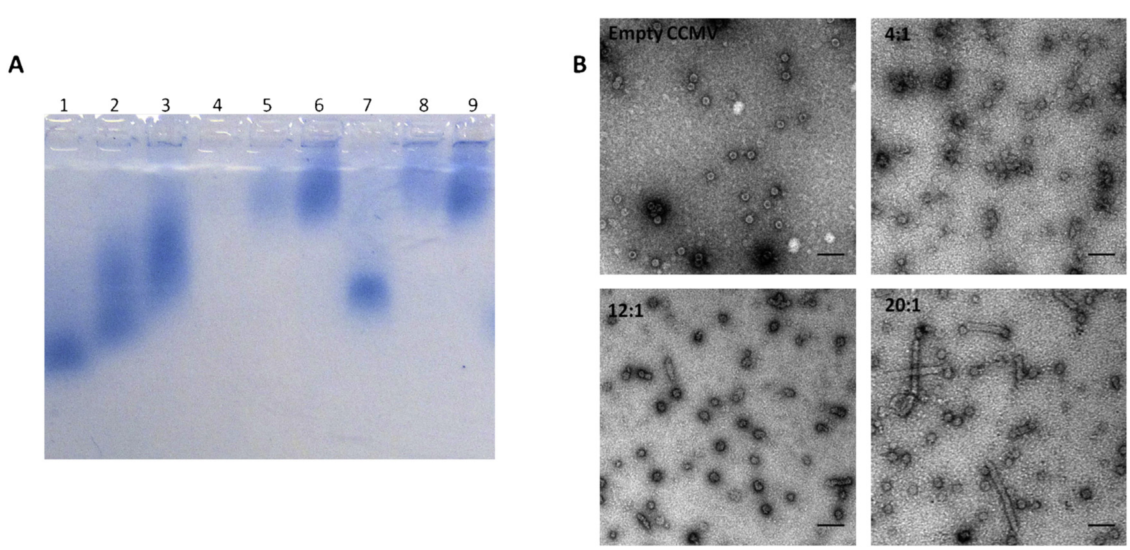


**Fig. 3.** CCMV:CYP assembly titrations. (A) Gel retardation assays using a 1% agarose gel stained with Instant Blue. Well 1 = 4:1 (9 μM CCMV coat protein:2.25 μM CYP); well 2 = 12:1 (27 μM CCMV coat protein:2.25 μM CYP); well 3 = 20:1 (45 μM CCMV coat protein:2.25 μM CYP); well 4 = 9 μM CCMV coat protein; well 5 = 27 μM CCMV coat protein; well 6 = 45 μM CCMV coat protein; well 7 = free CYP; well 8 = CCMV monomers; well 9 = empty CCMV VLP. (B) Transmission electron microscopy images of empty CCMV capsid and three CYP encapsulations at different protein ratios. Grids were negatively stained with uranyl acetate. Scale bar = 100 nm. (For interpretation of the references to color in this figure legend, the reader is referred to the web version of the article.)

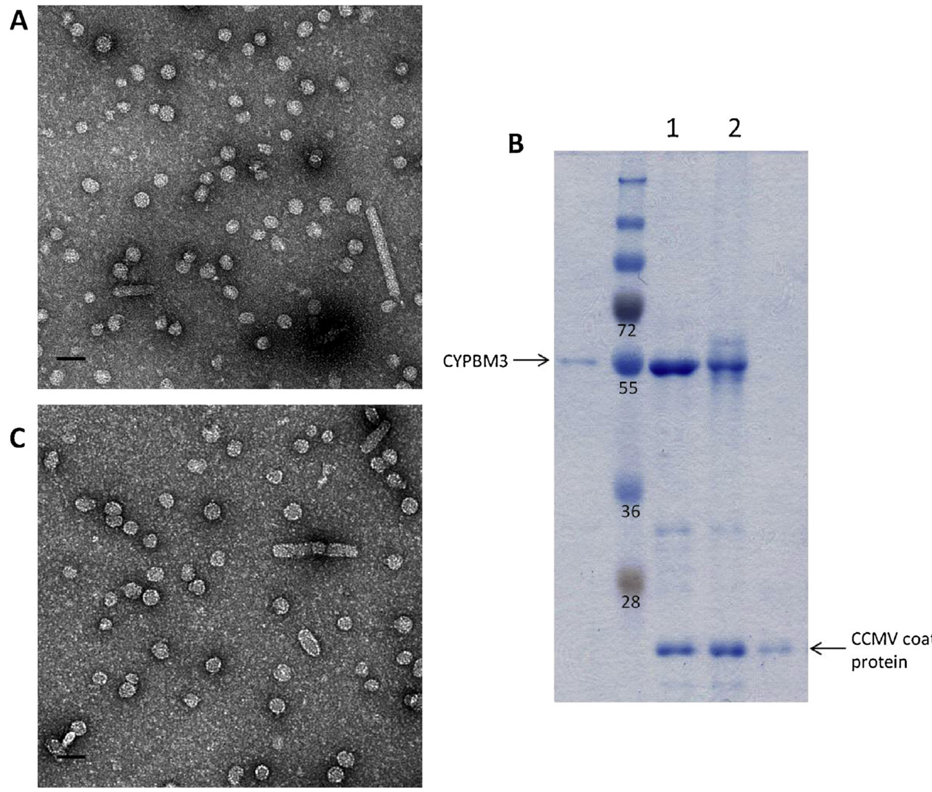


**Fig. 4.** Characterization of CCMV-CYP VLPs. (A) TEM image of the CCMV-CYP VLPs stained with uranyl acetate. Scale bar = 50 nm. (B) Electrophoretic analysis by 12% SDS–PAGE of CCMV-CYP encapsulation. Well 1 = 12:1 assembly; well 2 = 12:1 assembly after incubation in the presence of 5 mM $H_2O_2$. $CYP_{BM3}$ (55 kDa) and CCMV coat protein (19.8 kDa). Instant Blue staining. (C) Stability of CCMV-CYP VLPs after incubation in the presence of 5 mM $H_2O_2$. Scale bar = 50 nm. (For interpretation of the references to color in this figure legend, the reader is referred to the web version of the article.)

the external surface of the capsid. No genetic or chemical modifications, that could compromise the assembly of the capsid subunits, nor the structure (proper folding) of the enzyme, to either the viral protein or the enzyme were needed.

Finally, the transformation capacity of the catalytic VLPs was measured using the pro-drug tamoxifen as a substrate. This enzymatic activity (3.58 $min^{-1}$ or 65 nmol mg $protein^{-1}$ $min^{-1}$) is one order of magnitude lower compared to the activity of the free enzyme. This behavior has been reported for other encapsulated enzymes [16,25], and has been mainly attributed to crowding deleterious effects when working with a concentration of enzyme at the millimolar range, as in our case. Other factor that can be related to the activity decrease is the substrate diffusion into the VLP cavity. The 2 nm pores present in the CCMV capsid could be obstructed to a certain degree by the CYP molecules affecting the diffusion rate of the substrate into the nanoreactor. In addition, the orientation of the active site of the enzyme could also have detrimental effects on the CYP activity. It is important to point out that the CCMV-CYP VLPs are stable and maintain their structure when 5 mM of $H_2O_2$ is present, which is necessary for catalysis (Fig. 4C). Nevertheless, the tamoxifen transformation rate of the encapsulated CYP is similar than those from human and animal microsomal preparations. Human cDNA-expressed CYPs (CYP 2B6, 2C9, 2C19 and 2D6) and co-expressed with NADPH-P450 reductase in an insect cell line showed tamoxifen transformation rates, depending the CYP, from 30 to 760 $min^{-1}$ [53], which are similar to the obtained values in this work for the free CYPBM3 21B3 (41.9 $min^{-1}$). For microsomal human liver preparations, and beside a considerable variability, the rates of products formation from tamoxifen transformation vary from 1.2 to 122 pmol mg $protein^{-1}$ $min^{-1}$ [54–56], and high transformation rates as 1.7 nmol mg $protein^{-1}$ $min^{-1}$ for N-desmethyl-tamoxifen production have been reported for human liver microsomes [57]. All these reported values are significantly lower than the tamoxifen transformation by our CCMV-CYP VLPs (65 nmol mg $protein^{-1}$ $min^{-1}$). Thus, from these data is clear that the tamoxifen transformation rate obtained with CCMV-CYP VLPs is comparable, if not better, than the values for microsomal transformations.

Despite this, our laboratory is making efforts through site-directed mutagenesis to improve CYP activity and stability, as reported recently [30]. The stability of $CYP_{BM3}$ 21B3 toward hydrogen peroxide was recently improved (increase in half-life), making it a more robust enzyme for potential applications.

One of the main limitations of using VLPs as nanocarriers seems to be the immunological response against the viral proteins. However, there are several strategies being developed to overcome this issue. There are many examples in which the immunological response has been drastically reduced by masking the protein epitopes with polyethylene glycol [58,59]. Another alternative is to attach “Self” peptides to the surface of the capsid to reduce macrophage uptake and clearance [60]. In the case of the CCMV capsid, it has been demonstrated that it is highly biocompatible *in vivo* [61], which makes CCMV VLPs highly attractive as drug delivery systems.

Here, $CYP_{BM3}$ 21B3 has proven to be an excellent CYP model for the proof of concept studies on the encapsulation of CYP activity inside virus-like nanoparticles, as the basis of enzyme delivery for pro-drug activation. It was expressed heterologously in great quantities as a soluble protein and it was able to metabolize two pro-drugs, one currently used on cancer treatment, to the pharmacologically active metabolites.

To the best of our knowledge, this work shows for the first time the VLP encapsulation of a highly relevant protein in the biomedical field. This represents the first step toward the generation of a VLP based enzyme delivery system, as an alternative to the proposed genetic therapy, in which CYP encoding genes are introduced in the tumor tissue [8]. The final goal is to make more efficient chemotherapy drugs activating them mainly in the target tissue avoiding the dramatic side effects and reducing the doses needed to achieve a therapeutic effect.

## Acknowledgments

This work was funded by the Mexican Council of Science and Technology (SEP-CONACYT 165633). The authors thank Rosa Roman, Dr. Lucia Perezgasga and Francisco Ruiz for their technical support.

## References


[1] Beaglehole R, Bonita R, Magnusson R. Global cancer prevention: an important pathway to global health and development. Public Health 2011;125:821–31.
[2] Al-Lazikani B, Banerji U, Workman P. Combinatorial drug therapy for cancer in the post-genomic era. Nat Biotechnol 2012;30:679–92.
[3] Moen EL, Godley LA, Zhang W, Dolan ME. Pharmacogenomics of chemotherapeutic susceptibility and toxicity. Genome Med 2012;4:90.
[4] Huttunen KM, Mahonen N, Raunio H, Rautio J. Cytochrome P450-activated prodrugs: targeted drug delivery. Curr Med Chem 2008;15:2346–65.
[5] Bièche I, Narjoz C, Asselah T, Vacher S, Marcellin P, Lidereau R, et al. Reverse transcriptase-PCR quantification of mRNA levels from cytochrome CYP1; CYP2 and CYP3 families in 22 different human tissues. Pharmacogen Genom 2007;17:731–42.
[6] Choudharya D, Janssona I, Schenkmana JB, Sarfarazib M, Stoilovb I. Comparative expression profiling of 40 mouse cytochrome P450 genes in embryonic and adult tissues. Arch Biochem Biophys 2003;414:91–100.
[7] Zhao Y-N, Zhang W, Chen Y-C, Fang F, Liu X-Q. Relative imbalances in the expression of catechol-O-methyltransferase and cytochrome P450 in breast cancer tissue and their association with breast carcinoma. Maturitas 2012;72:139–45.
[8] Chen L, Waxman DJ. Cytochrome P450 gene-directed enzyme prodrug therapy (GDEPT) for cancer. Curr Pharm Des 2012;8:1405–16.
[9] Palmer DH, Mautner V, Mirza D, Oliff S, Gerritsen W, van der Sijp JRM, et al. Virus-directed enzyme prodrug therapy: intratumoral administration of a replication-deficient adenovirus encoding nitroreductase to patients with resectable liver cancer. J Clin Oncol 2004;22:1546–52.
[10] Tychopoulos M, Corcos L, Genne P, Beaune P, de Waziers I. Virus-directed enzyme prodrug therpy (VDEPT) strategy for lung cancer using a CYP2B6/NADPH-cytochrome P450 reductase fusion protein. Cancer Gene Ther 2005;12:497–508.
[11] Hooker J, Datta A, Botta M, Raymond KM, Francis MB. Magnetic resonance contrast agents from viral capsid shells: a comparison of exterior and interior cargo strategies. Nano Lett 2007:2207–10.
[12] Hu YF, Zandi R, Anavitarte A, Knobler CM, Gelbart WM. Packaging of a polymer by a viral capsid: the interplay between polymer length and capsid size. Biophys J 2008;94:1428–36.
[13] Abbing A, Blaschke U, Grein S, Kretschmar M, Stark CMB, Thies MJW, et al. Efficient intracellular delivery of a protein and a low molecular weight substance via recombinant polyomavirus-like particles. J Biol Chem 2004;279:27410–21.
[14] Seebeck F, Woycechowsky K, Zhuang W, Rabe JP, Hilvert D. A simple tagging system for protein encapsulation. J Am Chem Soc 2006;128:4516–7.
[15] Comellas-Aragonès M, Engelkamp H, Claessen VI, Sommerdijk NAJM, Rowan AE, Christianen PCM, et al. A virus-based single-enzyme nanoreactor. Nat Nanotechnol 2007;2:635–9.
[16] Patterson D, Prevelige P, Douglas T. Nanoreactors by programmed enzyme encapsulation inside the capsid of the bacteriophage P22. ACS Nano 2012;6:5000–9.
[17] Verma I, Weitzman M. Gene therapy: twenty-first century medicine. Annu Rev Biochem 2005;74:711–38.
[18] Ren Y, Wong S, Lim L. Folic acid-conjugated protein cages of a plant virus: a novel delivery platform for doxorubicin. Bioconjugate Chem 2007;18:836–43.
[19] Singh S, Sharma A, Robertson GP. Realizing the clinical potential of cancer nanotechnology by minimizing toxicology and targeted delivery concerns. Cancer Res 2012;72:5663–8.
[20] Sultana S, Khan MR, Kumar M, Kumar S, Ali M. Nanoparticles-mediated drug delivery approaches for cancer targeting: a review. J Drug Target 2013;21:107–25.
[21] Lee A, Niu Z, Wang Q. Viruses and virus-like protein assemblies-chemically programmable nanoscale building blocks. Nano Res 2009;2:349–64.
[22] Strable E, Finn M. Chemical modification of viruses and virus-like particles. Curr Topic Microbiol Immunol 2009;327:1–18.
[23] Azizgolshani O, Garmann RF, Cadena-Nava R, Knobler CM, William M. Reconstituted plant viral capsids can release genes to mammalian cells. Virology 2013;441:12–7.
[24] Minten IJ, Nolte RJM, Cornelissen JJLM. Complex assembly behavior during the encapsulation of green fluorescent protein analogs in virus derived protein capsules. Macromol Biosci 2010;10:539–45.
[25] Fiedler J, Brown S, Lau JL, Finn MG. RNA-directed packaging of enzymes within virus-like particles. Angew Chem Int Ed 2010;49:9648–51.
[26] Minten IJ, Claessen VI, Blank K, Rowan AE, Noltea RJM, Jeroen JL, et al. Catalytic capsids: the art of confinement. Chem Sci 2011;2:358–62.
[27] Glasgow J, Caperhart S, Francis MB, Tullman-Ercek D. Osmolyte-mediated encapsulation of proteins inside MS2 viral capsids. ACS Nano 2012;6:8658–67.
[28] Inoue T, Kawano M, Takahashi R, Tsukamoto H, Enomoto T, Imai T, et al. Engineering of SV40-based nano-capsules for delivery of heterologous proteins as fusions with the minor capsid proteins VP2/3. J Biotechnol 2008;134:181–92.
[29] Cirino P, Arnold F. A Self-sufficient peroxide-driven hydroxylation biocatalyst. Angew Chem Int Ed 2003;42:3299–301.
[30] Vidal-Limón A, Águila S, Ayala M, Batista CV, Vazquez-Duhalt R. Peroxidase activity stabilization of cytochrome P450BM3 by rational analysis of intramolecular electron transfer. J Inorg Biochem 2013;122:18–26.
[31] Sawayama AM, Chen MMY, Kulanthaivel P, Kuo M-S, Hemmerle H, Arnold FH. A panel of cytochrome P450 BM3 variants to produce drug metabolites and diversify lead compounds. Chem Eur J 2009;1:11723–9.
[32] Cadena-Nava R, Comas-Garcia M, Garmann RF, Rao ALN, Knobler CM, Gelbart WM. Self-assembly of viral capsid protein and RNA molecules of different sizes: requirement for a specific high protein/RNA mass ratio. J Virol 2012;86:3318–26.
[33] Komatsu T, Yamazaki H, Shimada N, Nakajima M, Yokoi T. Roles of cytochromes P450 1A2, 2A6, and 2C8 in 5-fluorouracil formation from tegafur, an anticancer prodrug, in human liver microsomes. Drug Metab Dispos 2000;28:1457–63.
[34] Lewis BC, Mackenzie PI, Miners JO. Application of homology modeling to generate CYP1A1 mutants with enhanced activation of the cancer chemotherapeutic prodrug dacarbazine. Mol Pharmacol 2011;80:879–88.
[35] Martins I, Souza JO, Sanson AL, Vieira EP, Giusti-Paiva A. Simultaneous determination of cyclophosphamide and ifosfamide in plasma using SPE-HPLC-UV method. Lat Am J Pharm 2009;28:41–6.
[36] Kim DH, Ahn T, Jung H-C, Pan J-G, Yun C-H. Generation of the human metabolite piceatannol from the anticancer-preventive agent resveratrol by bacterial cytochrome P450 BM3. Drug Metab Dispos 2009;37:932–6.
[37] Hoskins JM, Carey LA, McLeod HL. CYP2D6 and tamoxifen: DNA matters in breast cancer. Nat Rev Cancer 2009;9:576–86.
[38] Osborne CK. Tamoxifen in the treatment of breast cancer. N Engl J Med 1998;339:1609–18.
[39] Johnson MD, Zuo H, Lee K-H, Trebley JP, Rae JM, Weatherman RV, et al. Pharmacological characterization of 4-hydroxy-N-desmethyl tamoxifen; a novel active metabolite of tamoxifen. Breast Cancer Res Treat 2004;85:151–9.
[40] Notley L, de Wolf C, Wunsch R, Lancaster R, Gillam E. Bioactivation of tamoxifen by recombinant human cytochrome P450 enzymes. Chem Res Toxicol 2002;5:614–22.
[41] Perez EA. Safety profiles of tamoxifen and the aromatase inhibitors in adjuvant therapy of hormone responsive early breast cancer. Ann Oncol 2007;18(Suppl. 8):26–35.
[42] Ingelman-Sundberg M. Genetic polymorphisms of cytochrome P450 2d6 (CYP2D6): clinical consequences; evolutionary aspects and functional diversity. Pharmacogenom J 2005;5:6–13.
[43] Athar M, Back JH, Tang X, Kim KH, Kopelovich L, Bickers DR, et al. Resveratrol: a review of preclinical studies for human cancer prevention. Toxicol Appl Pharmacol 2007;224:274–83.
[44] Piotrowska H, Kucinska M, Murias M. Biological activity of piceatannol: leaving the shadow of resveratrol. Mutat Res 2012;750:60–82.
[45] Kuo P-L, Hsu Y-L. The grape and wine constituent piceatannol inhibits proliferation of human bladder cancer cells via blocking cell cycle progression and inducing Fas/membrane bound Fas ligand-mediated apoptotic pathway. Mol Nutr Food Res 2008;52:408–18.
[46] Morales P, Haza AI. Selective apoptotic effects of piceatannol and myricetin in human cancer cells. J Appl Toxicol 2012;32:986–93.
[47] Burke MD, Thompson S, Weaver RJ, Wolf CR, Mayer RT. Cytochrome P450 specificities of alkoxyresorufin O-dealkylation in human and rat liver. Biochem Pharm 1994;48:923–36.
[48] Aniagyei SE, DuFort C, Kao CC, Dragnea B. Self-assembly approaches to nanomaterial encapsulation in viral protein cages. J Mater Chem 2008;18:3763–74.
[49] Lavelle L, Gingery M, Phillips M, Gelbart WM, Knobler CM, Cadena-Nava RD, et al. Phase diagram of self-assembled viral capsid protein polymorphs. J Phys Chem B 2009;113:3813–9.
[50] Mukherjee S, Pfeifer CM, Johnson JM, Liu J, Zlotnick A. Redirecting the coat protein of a spherical virus to assemble into tubular nanostructures. J Am Chem Soc 2006;128:2538–9.
[51] Speir JA, Munshi S, Wang G, Baker TS, Johnson JE. Structures of the native and swollen forms of cowpea chlorotic mottle virus determined by X-ray crystallography and cryo-electron microscopy. Structure 1995;3:63–78.
[52] Cadena-Nava RD, Hu Y, Garmann RF, Ng B, Zelikin AN, Knobler CM, et al. Exploiting fluorescent polymers to probe the self-assembly of virus-like particles. J Phys Chem B 2011;115:2386–91.
[53] Hu Y, Dehal SS, Hynd G, Jones GB, Kupfer D. CYP2D6-mediated catalysis of tamoxifen aromatic hydroxylation with an NIH shift: similar hydroxylation mechanism in chicken, rat and human liver microsomes. Xenobiotica 2003;33:141–51.

[54] Crewe HK, Ellis SW, Lennard MS, Tucker GT. Variable contribution of cytochromes P450 2D6, 2C9 and 3A4 to the 4-hydroxylation of tamoxifen by human liver microsomes. Biochem Pharmacol 1997;53:171–8.
[55] Coller JK, Krebsfaenger N, Klein K, Endrizzi K, Wolbold R, Lang T, et al. The influence of CYP2B6, CYP2C9 and CYP2D6 genotypes on the formation of the potent antioestrogen Z-4-hydroxy-tamoxifen in human liver. Br J Clin Pharmacol 2002;54:157–67.
[56] Coller JK, Krebsfaenger N, Klein K, Wolbold R, Nüssler A, Neuhaus P, et al. Large interindividual variability in the in vitro formation of tamoxifen metabolites related to the development of genotoxicity. Br J Clin Pharmacol 2003;57:105–11.
[57] Desta Z, Ward BA, Soukhova NV, Flockhart DA. Comprehensive evaluation of tamoxifen sequential biotransformation by the human cytochrome P450 system *in vitro*: prominent roles for CYP3A and CYP2D6. J Pharmacol Exp Ther 2004;310:1062–75.
[58] Kreppel F, Kochanek S. Modification of adenovirus gene transfer vectors with synthetic polymers: a scientific review and technical guide. Mol Ther 2008;16:16–29.
[59] Oh IK, Mok H, Park TG. Folate immobilized and PEGylated adenovirus for retargeting to tumor cells. Bioconjugate Chem 2006;17:721–7.
[60] Rodriguez PL, Harada T, Christian DA, Pantano DA, Tsai RK, Discher DE. Minimal self peptides that inhibit phagocytic clearance and enhance delivery of nanoparticles. Science 2013;339:971–5.
[61] Kaiser CR, Flenniken ML, Gillitzer E, Harmsen AL, Harmsen AG, Jutila MA, et al. Biodistribution studies of protein cage nanoparticles demonstrate broad tissue distribution and rapid clearance *in vivo*. Int J Nanomed 2007;2:715–33.